HMG Advance Access published August 5, 2015

A NEW VARIANT IN SIGNAL PEPTIDE OF THE HUMAN LUTEINIZING HORMONE RECEPTOR (*LHCGR*) AFFECTS RECEPTOR BIOGENESIS CAUSING LEYDIG CELL HYPOPLASIA

Valeria Vezzoli[1,2,#], Paolo Duminuco[2,#], Alessandra Vottero[3], Gunnar Kleinau[4], Ralf Schülein[5], Roberta Minari[3], Ivan Bassi[2,6], Sergio Bernasconi[3], Luca Persani[1,2], Marco Bonomi[1,2,*]

[1]Dipartimento di Scienze Cliniche e di Comunità, Università di Milano, Milano, MI, Italy

[2]Divisione di Medicina Generale ad Indirizzo Endocrino-Metabolico e Laboratorio di Ricerche Endocrino-Metaboliche, Istituto Auxologico Italiano IRCCS, Cusano Milanino, MI, Italy

[3]Dipartimento di Medicina Clinica e Sperimentale, Università degli Studi di Parma, Parma, Italy

[4]Institute of Experimental Pediatric Endocrinology, Charité-Universitätsmedizin, Berlin, Germany

[5]Leibniz-Institut für Molekulare Pharmakologie (FMP), Berlin, Germany

[6]Dipartimento di Scienze della Salute, Università di Milano, Milano, MI, Italy

[*]Corresponding author: Marco Bonomi, MD, Dipartimento di Scienze Cliniche e di Comunità, Università degli studi di Milano, IRCCS Istituto Auxologico Italiano, Divisione di Medicina Generale ad Indirizzo Endocrino-Metabolico, Piazzale Brescia 20, 20149 Milano, Phone: +39-02619112390, Fax: +39-02619113033, email: marco.bonomi@unimi.it

[#]These authors contribute equally to this work

Abstract

The human luteinizing hormone/chorionic gonadotropin receptor (LHCGR) plays a fundamental role in male and female reproduction. In males, loss-of-function mutations in LHCGR have been associated with distinct degrees of impairment in pre- and postnatal testosterone secretion resulting in a variable phenotypic spectrum, classified as Leydig cell hypoplasia (LCH) type 1 (complete LH resistance and disorder of sex differentiation) and type 2 (partial LH resistance with impaired masculinization and fertility).

Here, we report the case of an adolescent who came to the pediatric endocrinologist at the age of 12 years old for micropenis and cryptorchidism. Testis biopsy showed profound Leydig cell hypoplasia and absent germinal line elements (Sertoli-only syndrome). The sequence analysis of the *LHCGR* gene showed the presence of a compound heterozygosity, being one variation, c.1847C>A p.S616Y, already described in association to Hypergonadotropic Hypogonadism (HH), and the other, c.29 C>T p.L10P, a new identified variant in the putative signal peptide of LHCGR. Functional and structural studies provide first evidence that LHCGR have a functional and cleavable signal peptide required for receptor biogenesis. Moreover, we demonstrate the pathogenic role of the novel p.L10P allelic variant, which has to be considered a loss-of-function mutation significantly contributing, in compound heterozygosity with p.S616Y, to the Leydig cell hypoplasia type 2 observed in our patient.

Introduction

The human luteinizing hormone/chorionic gonadotropin receptor (*LHCGR*: OMIM #52790) belongs to the class A G-protein-coupled receptor, and consists of 699 amino acid with a molecular weight of 85-95KDa (1). Its gene is located on chromosome 2p21 and consists of 12 exons. Exons 1–10 and a part of exon 11 encode for the extracellular domain (ECD), which is responsible for ligand binding. The remaining exon 11 encodes for the transmembrane domain consisting of seven helices (TMH) and the intracellular C-terminal tail, which are involved in signal transduction (2,3). The LHCGR transduces intracellular signaling cascades upon activation by the pituitary luteinizing hormone (LH) or the placental human chorionic gonadotrophin (hCG). Its role is fundamental in male and female fetal sex differentiation and reproductive physiology (4). Indeed, homozygous or compound heterozygous loss-of-function mutations in the *LHCGR* gene have been described in males and females and have provided important insights into distinct physiological roles of LH in reproduction of both sexes (5). Depending on the severity of the LHCGR inactivation, a variable spectrum of disorders of sex differentiation (DSDs) has been described (6). In Leydig cell hypoplasia (LCH, OMIM #238320), male to female DSD and absence of sexual maturation at puberty are the phenotypic features of 46,XY patients with the severe form of LHCGR resistance, also called LCH type 1. Patients with milder forms of resistance, LCH type 2, have micropenis and/or hypospadias or only infertility without sexual ambiguity. These patients present low testosterone levels unresponsive to the rise of endogenous LH concentrations after pubertal age or to exogenous hCG stimulation associated to only slight reduction in testes size but with variable LCH. Currently, more than 30 LHCGR variants have been identified with variable loss-of-function (1). These inactivating variations are scattered throughout the different domain of the LHCGR, either the ECD or the TMH or the C-terminal tail. Very recently a 27 bp deletion was detected in exon 1 at amino acid number 12 involving the signal peptide region of the LHCGR (7). Nevertheless, no specific functional studies were provided in this report regarding the role of the LHCGR signal peptide. Here, we report a new case of LCH type 2 due to a biallelic defect in the *LHCGR* gene. One substitution, p.S616Y, was previously described in a patient with LCH (8), while the second one, p.L10P, is a novel substitution located in the putative signal peptide of LHCGR. In this work, we have functionally characterized the LHCGR receptor signal peptide and the impact of p.L10P substitution. We show that the signal peptide of LHCGR is indeed necessary for receptor expression and trafficking, but not for the formation of a functional receptor entity and

that p.L10P variant strongly impair receptor biogenesis.

Results

3.1 Patient characterization and genetic analysis

The patient, a 46 XY male, presented at birth with micropenis, cryptorchidism and hypospadias. At 5 years of age, he underwent surgery for bilateral cryptorchidism. At 12 years, he came to the pediatric endocrinologist for the evaluation of auxological parameters and pubertal development: his height was >97°percentile and weight >97°percentile, the Tanner stage was PH3 with a testicular volume of 4 ml bilaterally and defective penis length (2 cm; <2.5 SDS for age). Hormonal evaluation showed prepubertal total Testosterone (T <0.69 nmol/L) with slight elevation of gonadotropin levels (LH=10.9 IU/L; FSH=6.5 IU/L), and an exaggerated response of LH to GnRH test and a poor increase of T to hCG stimulation (see Fig.1A). A second evaluation at the age of 15 years showed primary hypogonadism (LH=40.8 IU/L; FSH=16.0 IU/L; total T= 4.09 nmol/L, Fig.1A). No other hormonal deficiencies were present. Testis biopsy showed profound Leydig cell hypoplasia and absent germinal cells. The sequence analysis of the *LHCGR* gene showed the presence of a compound heterozygosity: one variation, c.1847C>A (p.S616Y), was previously described in association to LCH (8,9), and the other, c.29 C>T (p.L10P), revealed to be a new variant (Fig.1B).

Investigations in the family, revealed that the two parents were heterozygous carriers of the two variants, with paternal allele encoding the p.S616Y variant and the maternal allele carrying the new variant. The normal phenotype of the parents indicates that one functional allele of the LHCGR gene is sufficient for normal LHCGR function and reproductive processes.

3.2 The p.L10P variant do not completely abolish LHCGR activity but affect receptor expression

In a cAMP stimulation assay on COS7 cells transfected with the wild type (WT) LHCGR or p.L10P variant, the cells expressing the p.L10P construct respond to hCG with a reduced Emax (to 58.6% of the WT level) and an equal EC_{50} (0.063 IU/L versus 0.064 IU/L) in comparison with the wild-type LHCGR (Fig.2A).

The level of receptor expression on the cell surface was then investigated by immunofluorescence, using a specific antibody directed against a linear epitope mapping in the LHCGR ECD, but far from the N-terminal domain where is located the mutant p.L10P. As shown in Fig. 2B, the wild type LHCGR is correctly expressed and trafficked on the cell surface, whereas the L10P substitution results in a significant reduction of receptor expression level. The WT LHCGR expression was also quantified through flow cytometry in non-

permeabilized cells (Fig.2C) and we show that the cell surface amount of the p.L10P mutant is largely reduced to 14.6 ± 2.17% ($P < 0.001$, ANOVA) of the WT receptor. Similarly, the total receptor expression amount of p.L10P in permeabilized cells (Fig.2D) is drastically impaired (26.3 ± 1.34% ($P < 0.001$, ANOVA) of the WT receptor), while the total receptor expression of p.S277L variant, already known to be an intracellular retained mutant (10), is similar to WT. The ratios between membrane associated/intracellular receptors (panel 2E) are consistent with a prevalent trafficking defect for p.S277L and a prevalent synthesis defect for p.L10P.

Finally the LHCGR expression was tested by Western blot experiments in COS7 transfected cells. Using a specific antibody directed against the C-terminal domain of LHCGR, two bands of the expected molecular size (Fig.2E, lane 2) can be seen in total homogenates of COS7 transfected with the WT receptor. The amount of these two different receptor isoforms is drastically reduced (up to 80%, Fig.2F) in total homogenates of cells transfected with p.L10P mutant.

3.3 The putative signal peptide of LHCGR is functional and cleavable

Because the p.L10P mutation is located in the hydrophobic region of the putative signal peptide of *LHCGR*, the decreased receptor activity and expression may result from an altered function of the signal peptide itself. Signal peptides of membrane proteins are predictable by computer programs such as *SP Scan* (Genetics Computer Group, Madison, WI, U.S.A.). The human LHCGR receptor contains a putative signal peptide when monitored with the program "Signal IP 3.0" (11,12) (Fig.3A). The likelihood of the identified signal peptide in WT receptor sequence is very high (0.966) and the maximal cleavage site probability (cp) occurs between residues Ala24 and Leu25 (probability: 0.662). According to the computational analyses, the p.L10P substitution affects both of the above mentioned parameters: signal peptide and maximal cleavage site probability are decreased at 0.702 and 0.286, respectively.

To assess whether the putative signal peptide of the LHCGR receptor is functional, the sequence for the N tail of the receptor with signal peptide was fused with a His-tagged GFP as a soluble marker protein. Constructs containing the N tail of the CRF-R1 (Corticotropin-Releasing Factor Receptor 1) and CRF-R2a (Corticotropin-Releasing Factor Receptor 2a) were used as positive and negative controls, respectively. Alken and colleagues (13) report that if a cleavable signal peptide is present in the N-terminal domain of the LHCGR receptor, it should direct the soluble GFP marker to the endoplasmic reticulum (ER) and subse-

quently via the secretory pathway to the cell culture medium. On the opposite, if the sequence does not contain a functional signal peptide, the marker protein is expected to remain in the cytosol. According to this approach, we transiently transfected COS7 cells with these constructs and the GFP fluorescence signals were localized by confocal LSM (Fig.3B). In case of the WT LHCGR receptor and CRF-R1 positive control, reticular signals and a GFP-free nucleus (Fig.3B) can be detected, indicating that the fusion protein is directed to the ER membrane and into the ER lumen. Moreover the presence of the GFP protein in the cell culture medium (Fig.3C) shows that the N-terminal domain of LHCGR contains a cleavable signal peptide. In contrast, cytosolic and nuclear GFP signals are seen in the case of p.L10P mutant and CRF-R2a negative control, indicating that the mutant signal peptide is unable to mediate ER targeting/insertion of heterologous proteins.

3.4 Specific mutations at position 10 of the LHCGR signal peptide are not predicted to disturb the secondary structure

The potential effect of the p.L10P mutation on the LHCGR structure was estimated by assembling a complex model between the signal recognition particle protein (SRP) and the signal peptide of the LHCGR.

SRP proteins include three domains: the N-terminal four-helix bundle (N domain), a Ras-like GTPase domain (G domain), and the carboxy-terminal methionine-rich (M-) domain (Fig.4A) that associates with SRP-RNA and the signal peptide (SP) sequence (14).

Three subsequent portions (the n-, the h- and the c-region) generally constitute the signal peptides (see Fig.4A). Amino acids in the h-region of the signal peptide (Fig.4A) are in a α-helical conformation, but the helix probably extends to Arg23, with a bend at Pro19 and Pro20. It's worth noting that three glutamates of the SRP M domain are interacting in complementation with positively charged residues of a M domain loop structure and arginines of the LHCGR SP C-terminus (Fig.4A). The p.L10P substitution is located at the transition between the n- and the h-region of the SP. The n-region includes also few hydrophilic residues like Gln9, which can interact with a glutamine at the SRP M domain. However, the hydrophobic part of the SP is likely responsible for the correct relative orientation of the components (15). This orientation is finally also critical for justifying of the M domain relative to the exit channel in the ribosome. The simulated substitution of Leu10 to Pro10 in a complexed SRP/SP structure results only in a slight modification of the SP backbone, however proline substitutions are known to induce structural modifications like helix-kinks (16). In order to

asses and to distinguish if changes in biophysical properties or structural prerequisites at this position are critical for the SP function, we created three additional “in silico” variants and experimentally tested the expression of the mutated LHCGR receptor by western blot analyses. A marked reduction of receptor expression is observed also when the leucine at position 10 is substituted by the polar amino acid serine (Fig.4B). Indeed the p.L10S substitution should lead to different SRP/SP interaction pattern, like with hydrophilic amino acids at the M domain, which would finally cause a dis-arrangement of the general complex architecture. We therefore conclude, that the change in biophysical properties like hydrophobicity at this position is responsible for observed dysfunction, rather than drastic changes in the secondary SP structure.

3.5 The pL10P variant is recovered by MG132 treatment

Typically, a cleavable signal peptide mediates ER targeting/insertion of the nascent chains. Therefore, the reduced expression of the p.L10P mutant may result either from an impaired ER targeting/insertion of the receptor with an abnormal signal peptide, or from decreased transcription or translation. To exclude the latter alternative, we performed Real Time PCR experiments with total RNA derived from transiently transfected COS7 cells (Fig.5A). Both transcripts were present in similar amounts, demonstrating that differences in transcription do not account for the reduced expression of the signal peptide mutant.

Taken together, our results indicate that the signal peptide of LHCGR improves one of the early steps of receptor biogenesis such as targeting and/or insertion. We thus speculate that the p.L10P substitution could impair receptor biogenesis leading to a premature degradation of the immature receptor. To test this hypothesis, COS7 cells transfected with the wild type and the p.L10P construct were treated with the proteasome inhibitor MG132 24 hours after transfection. Accordingly, treatment with MG132 leads to accumulation of a lower molecular weight form (approximatively 65 kDa) in cells transfected with the p.L10P mutant compared to the WT counterpart (Fig 5B). Moreover, immunofluorescence experiments shows the appearance of an intracellular signal in cells transfected with the construct p.L10P following the treatment with the proteasome inhibitor MG132 (Fig 5C). To further investigate the nature of this lower molecular weight form, the lysates of MG132-treated cells were digested with PNGaseF, a glycosidase that removes all types of N-linked glycans (Fig 5D). In accordance with previous published data (17), PNGaseF treatment affects electrophoretic mobility of the two distinct WT-LHCGR species leading to the accumulation of a ~ 62 KDa lower band. On the contrary, the PNGaseF treatment does not affect the molecular weight of the ~65-kDa band

observed in cells transfected with the p.L10P, indicating that the p.L10P protein should not be able to translocate into the ER lumen but is rather located in the cytosol, where it cannot be glycosylated in accordance with the GFP targeting experiments. Furthermore, the shift of the two different molecular species of WT-LHCGR to a smaller size (~ 62 KDa) indicates that this protein species has undergone signal peptide cleavage, whereas the p.L10P 65-kDa fragment has not.

Discussion

We describe the functional impact of the new p.L10P substitution in the signal peptide of LHCGR that was found in a male adolescent with LCH type 2. The sequence analysis of the *LHCGR* gene in this patient revealed a compound heterozygosity, between p.S616Y and p.L10P inherited from the unaffected heterozygous mother and father, respectively. Indeed, the in vitro results here shown, including the experiments after co-expression of the different LHR isoforms (wt and/or L10P and/or S616Y) (see Supplemental Figure 1), correlate well with the clinical expression of the disease in the family. Because the p.L10P insertion is located in the hydrophobic region of the putative signal peptide of LHCGR, we thought that the decreased receptor activity and expression (Fig.2A-D) might result from an altered function of the signal peptide itself.

Few data are presently available on the role of the signal peptide in the GPCR field. One possible role is to mediate the translocation across the ER membrane if the N-terminal domain of a receptor cannot be translocated post-translationally, as previously reported for the endothelin B receptor (18). Removal of such a signal peptide leads to abnormally folded and non-functional receptors. A second role, as described for CRF-R1, is to modulate receptor expression by a still incompletely understood mechanism (13). In the CRF-R1, the signal peptide precedes the N-terminal domain that can be translocated post-translationally, but it is not required for the formation of a functional receptor.

In the present study, we provide a functional characterization of the cleavable signal peptide in LHCGR. We show that an abnormal signal peptide does not completely abolish the LHCGR activity as both the wild-type and the SP-mutant receptors were able to stimulate the adenylate cyclase system without significant changes in the EC_{50} (0,064 versus 0,063 IU/L) (Fig.2A). However, the signal peptide has a strong impact on receptor expression. Western blot experiments, FACS analysis and confocal laser scanning microscopy (Fig.2B-D) consistently revealed that expression of the p.L10P mutant is decreased by 70-80%. Since a mechanism for specific mRNA degradation in response to the synthesis of defective proteins was recently reported (13,19),

we have also excluded the possibility that the sequence encoding the signal peptide has an effect on mRNA level or translation efficiency (see Fig.5A).

Thus the LHCGR signal peptide influences one of the processes of the early secretory pathway. It may facilitate targeting of the nascent chain–SRP–ribosome complex to the ER membrane or alternatively prevent an early degradation process. We explored the potential effect of this mutation on the protein structure assembling by a structural homology complex between the signal recognition particle protein (SRP) and the signal peptide of the LHCGR. The simulated substitution of Leu10 to Pro10 in a complexed SRP/SP structure results only in a slight modification of the SP backbone. However, based on insights from the model in combination with mutagenesis studies (e.g. Leu10Ser) we speculate, that the change in biophysical properties like hydrophobicity at this position has effects on component justification (de-justification), which is likely responsible for the SP malfunction in the interaction with the SRP.

Typically, the signal peptide sequence is co-translationally recognized by SRP (20). The ribosome-nascent chain-SRP complex is targeted to its receptor in the ER membrane where the nascent chain is translocated into ER lumen by the Sec61p/TRAM translocon, and finally the signal sequence is removed by signal peptidase (13,21-23). Based on our data, we hypothesize that the p.L10P mutation causes a disarray in the assembling of the SRP/SP complex, thus interfering with the translocation of the nascent receptor chain into ER lumen.

The experiments addressing signal peptide functionality of the p.L10P mutant strongly suggest that its signal peptide is completely non-functional. However, the cAMP accumulation assay revealed that minor amounts of the mutant are nevertheless present at the plasma membrane. On the one hand, these results indicate that the signal peptide of the LHCGR is not an absolute requirement for a functional receptor similar to the signal peptide of the CRF-R1 previously described (13). On the other hand, these results raise the question on the rescue mechanism allowing minor amounts of the p.L10P mutant to reach the ER and consequently the plasma membrane. In the absence of a functional signal peptide, the transmembrane segment 1 (TM1) of the receptor could take over the ER targeting/insertion functions as a signal anchor sequence. In the case of the p.L10P mutant, one may speculate that a small ancillary functional population could be successfully integrated into the ER membrane by the signal anchor sequence mechanism and reach the plasma membrane. This might be also dependent on the fact that we are working in heterologous cell system with an overex-

pression of the mutant receptor and not in the natural host cells. However our data suggest that both ER targeting/insertion or N tail translocation are mainly defective also by using such rescue mechanism. In the case of the p.L10P mutant the larger receptors population may not even reach the ER membrane or may be misfolded due to an impaired N-terminal domain translocation. These receptors would be present in their non-glycosylated form in the cytosol, rapidly degraded by the proteasome and consequently stabilized by MG132 treatment (Fig.5C).

In conclusion, we provide the first experimental evidences that LHCGR have a functional and cleavable signal peptide required for receptor biogenesis. Moreover, our *in vitro* results demonstrate the pathogenic role of the novel p.L10P allelic variant, which is to be considered a novel loss-of-function mutation significantly contributing, in compound heterozygosity with the p.S616Y mutation, to the Leydig cell hypoplasia type 2 observed in our patient.

Materials & Methods

2.1. DNA isolation and sequencing analysis

Genomic DNA from the patient and his parents was extracted from peripheral blood using the QIAamp DNA Blood Mini Kit (Qiagen Inc., Valencia, CA, USA) and stored at –20°C until use. Written informed consent was obtained from all the subjects. Exons of the LHCGR gene (GeneBank accession number NM_000233.3) were amplified by PCR with intron spanning primers as previously described (24). Genomic DNA was sequenced using a CEQ Dye-Terminator Cycle Sequencing kit (Beckman Coulter Inc., Miami, FL, USA) according to the manufacturer's protocol. Sequence alignments were performed with DNAStar program (DNAStar Inc., Madison, WI, USA). Sequences with DNA variations were confirmed from a separately DNA extraction, PCR amplification and sequence reaction. All the sequence reactions were performed using a CEQ XL2000 DNA Analysis System (Beckman Coulter).

2.2 Mutant expression vectors

Plasmid pSVL-hLHCGR (25) was a generous gifts from Dr. Sabine Costagliola (IRIBHM, Bruxelles, Belgium) and it is based on the receptor sequence published by Minegishi et al (Minegishi et al, 1990; Rodien P et al, 1998). Restriction enzymes were from New England Biolabs (Beverly, MA, USA); Pfu Turbo polymerase was from Stratagene (La Jolla, CA, USA). Go Taq polymerase from Promega (Madison, WI, USA). Purified hCG was obtained from Sigma (Sigma Chemical CO, St Louis, MO, USA). The pSVL-hLHCGR

vector was then used as template to introduce the allelic variant p.L10P by QuickChange (Stratagene; La Jolla, CA, USA) site-direct mutagenesis method using specific oligonucleotides.

Plasmids pCRF1 and pCRF2A were a generous gift of Prof. Ralf Schuelein. These vectors encode GFP fusions to the N tail of the CRF1 and CRF2A receptor (position Ala121) with signal peptide, respectively, in the vector pSecTag2A. In the case of the LHCGR, the N terminal sequence of the wild type and p.L10P signal peptide mutant (position 66) replace the N tail of the CRF1 in the pCRF1plasmid before the GFP sequence. An additional C-terminal His6 sequence in all four constructs allows the purification of the GFP fusions.

2.3 Mutant Expression and functional studies

Signal transduction- For cAMP determinations COS7 cells were seeded in 3.5 cm dishes and used 48h post-transfection with FUGENE HD (Promega Corporation, Madison, WI, USA). Experiments were run in duplicates dishes and repeated at least three folds. For intracellular cAMP level determinations we used a previously described method (25) using various concentration of purified hCG as stimulus. The results are expressed as fold of the WT. Concentration-effect curves were fitted with GraphPad Prism 5.0 (GraphPad Software, Inc., San Diego, CA), and EC50 values were determined.

Fluorescence-activated cell sorting (FACS) analysis- COS7 cells seeded in 3.5 cm dishes were used 48h post-transfection with 1µg of DNA (FUGENE HD). The immunoreactivity of transfected cells was determined after fixing them for 10 min on ice with 1% paraformaldehyde and treatment (only for permeabilized cells) with 0.2% saponine for 30 min at RT. Receptor expression was determined by using the 4G2 monoclonal antibody and the fluorescine-conjugated γ-chain-specific goat antimouse IgG (Sigma, St. Louis, MO, USA) as secondary antibody. The monoclonal antibody (mAb) 4G2 was obtained by genetic immunization with the cDNA coding for the hLHCGR (Bonomi et al, unpublished results) as previously described (Costagliola et al, BBRC, 2002) and it is directed against a linear epitope in the C-terminal portion of LHCGR ECD, between the aminoacid 317 and 356. The fluorescence of 10,000 cells/tube was assayed by a FACScan flow cytofluorometer (Becton Dickinson and Co., Franklin Lakes, NJ, USA).

Immunocytochemistry- COS7 cells were plated (1×10^5) on sterile coverslips placed in 35 mm Petri dishes and transfected with 1 µg of DNA. 24 hours after transfection, cells were washed with PBS, fixed with PBS containing 3% paraformaldehyde (Sigma-Aldrich St. Louis, MO, USA) for 10 min at room temperature and

rinsed twice with PBS. Cells were permeabilized with 0,1% Triton X-100 (Sigma-Aldrich, St. Louis, MO, USA), blocked with 5% goat serum (Invitrogen, Auckland, NZ), incubated with primary antibody 1:10 in goat serum (4G2) overnight at 4°C and incubated with the appropriate secondary antibodies (Alexa Fluor 488 goat anti-mouse IgG, Life Technologies, Carlsbad, CA, USA) 1:1000 for 1 h at room temperature. Finally cells were mounted with SlowFade Gold antifade reagent with Dapi (Life Technologies, Carlsbad, CA, USA). Images were acquired by using a laser scanning confocal system installed on a Nikon Eclipse Ti microscope with a 60X oil immersion objective. Alexa Fluor 488 was excited with a 488-nm argon laser and detected with a 525–550-nm band pass filter.

Western Blotting- COS7 cells were plated (1×10^5) in 35 mm Petri dishes and transfected with 1µg of DNA. 48h after transfection, cells were washed with PBS and suspended in 200 µl of RIPA Buffer (10 mM Tris-HCl pH 7,2, 150 mM NaCl, 0,1% SDS, 1.% Triton X-100, 1% sodium deoxycholate, 5 mM EDTA) supplemented with protease inhibitors and lysed using a syringe with a small gauge needle. Homogenates were centrifuged at 4000 x g for 10 min at 4 °C to remove cell debris. Protein content was assayed by the BCA protein Assay Kit (Pierce, Rockford, IL 61101 USA). Total proteins were fractionated by SDS electrophoresis on NuPage 4-12 % Bis-Tris gel (Life Technologies) and electrotransferred onto nitrocellulose membranes (Hybond-C super, Amersham Biosciences, Bucks HP97 9NA, UK). After blocking with TBS supplemented with 5% non-fat dry milk and 0.1% Tween 20, membranes were incubated overnight at 4 °C with mAb 4G2 or anti-GAPDH (Santa Cruz Biotechnology sc-25778) as internal control. After three washings in TBS-0.1% Tween solution, membranes were incubated for 1 h at room temperature with a 1:10000 dilution of peroxidase-coupled goat anti-mouse antibody. Antibody-protein complexes were then detected using the Novex ECL Chemiluminescent substrate reagent kit (Life Technologies, Carlsbad, CA, USA) followed by autoradiography. For deglycosylation reactions with N-glycosidase F (PNGaseF), the manufacturer's instructions were followed (New England Biolabs, Westburg, Leusden, The Netherlands).

MG132 treatment-The proteasome inhibitor MG132 (Z-Leu-Leu-Leu-al, purity ~80% HPLC, Sigma-Aldrich St. Louis, MO, USA) was dissolved in DMSO (Sigma-Aldrich St. Louis, MO, USA) at 100 mM stock solution and stored at −20°C. COS7 cells were plated at 1×10^5 cells/well in 35mm Petri dishes or sterile coverslips placed in 35 mm dishes and transfected with 1µg of DNA. 24 hours after transfection, cells were treated with 10 µM of MG132 for different time points (from 8 up to 24 hours) or DMSO as control . Subse-

quently cells were washed with PBS and processed for immunocytochemistry and western blotting as previously described.

2.4 Quantitative detection of secreted GFP fusion proteins

Secreted GFP fusion proteins were analyzed by confocal laser scanning microscopy and immunoblotting. COS7 cells (1×10^5) grown on glass coverslips in 35-mm diameter dishes were transiently transfected with plasmid DNA (1 μg) and FUGENE HD according to the supplier's recommendations. Cells were incubated overnight, washed once with PBS, and mounted with SlowFade Gold antifade reagent with Dapi (Life Technologies, Carlsbad, CA, USA). Images were acquired by using a laser scanning confocal system installed on a Nikon Eclipse Ti microscope with a 60X oil immersion objective. Alexa Fluor 488 was excited with a 488-nm argon laser and detected with a 525–550-nm band pass filter.

COS7 cells (4×10^6) grown on 100 mm diameter dishes were transiently transfected with 6 μg of plasmid DNA and 20 μl of FUGENE HD. After 24h the cell-culture medium (8 ml) was collected and cell debris was removed by centrifugation (5 min, 200 g). TALON metal-affinity resin beads (500 μl bed volume) were washed twice with washing buffer (37 mM Na2HPO4, 11mM NaH2 PO4 and 300 mM NaCl, pH 7.0) and added to the cell-culture medium. The sample was incubated for 30 min to allow coupling of the His-tagged GFP fusion proteins with the beads. Resin beads were collected (2 min, 700 g), washed three times with washing buffer and resuspended in 200 μl of elution buffer (37 mM Na2HPO4, 11 mM NaH2PO4, 300 mM NaCl and 150 mM imidazole, pH 7.0). The GFP fusion proteins were solubilized for 15 min and the resin beads were separated by centrifugation as described above. For Western-blotting detection of the CRF1 secreted fusion proteins, 30 μl of the resulting supernatant was treated with PNGase F. The sample was supplemented with Laemmli buffer (60 mM Tris/HCl, 2%, w/v, SDS, 10%, v/v, glycerol, 5%, v/v, 2-mercaptoethanol and 0.1%, w/v, Bromophenol Blue, pH 6.8), incubated for 3 min at 95°C and proteins were analyzed by SDS/ PAGE/immunoblotting as previously described. Secreted proteins were detected with the polyclonal rabbit anti-GFP (Roche, 11814460001).

2.5 Real-time quantitative PCR (qPCR)

Total RNA was isolated from subconfluent (~90%) cells seeded in 10 cm diameter Petri dishes, by using a Qiagen RNeasy Protect Mini kit (Quiagen, Italy) according to manufacturer instructions. Total RNA concentration was spectrofotometrically quantified, and structural integrity of the RNA samples was confirmed by

electrophoresis in 1% Tris-borate-EDTA (TBE)-agarose gels. After digestion with DNAse I (Sigma-Aldrich, Italy), 2 µg of mRNA were retro-transcribed to cDNA via SuperScript II Reverse Transcriptase (Life Thecnologies, Italy). Real-time qPCR assays were performed in a 25 µl reaction volume containing 12.5 µl 2× SYBR Green I PCR Master Mix (Applied Biosystems, USA), 10 (actin) or 50 ng (all the other genes) cDNA, 10 µM forward and reverse primers. Reactions were performed in 96-well µultraAmp PCR Plates - FastPlate96 (Sorenson) using the ABI Prism 7900 high-throughput sequence detection systems (Applied Biosystems) and data were processed by the associated SDS software version 2.3 (Applied Biosystems).

For each gene an amplification curve was made to evaluate the amplification efficiency. The sequences of forward and reverse primers are: LHCGR forward primer 5'-ctgccgagctatggcctag-3'and reverse primer 5'-attctgttcttttgttggcaagtt-3'; GAPDH: forward primer 5'-gggaagcttgtcatcaatgga-3' and reverse primer 5'-cgccccacttgattttgg-3'.After each PCR, a melting curve was always made, to check for specificity of PCR.

2.6 Structural homology modeling of an SRP/LHCGR SP complex

To build a structural homology complex between the signal recognition particle protein (SRP) and the signal peptide (SP) of the LHCGR we used as a homology model-template the high resolution structure from Sulfolobus solfataricus in complex with a signal peptide from yeast dipeptidyl aminopeptidase B (pdb code 3KL4, PMID: 20364120, sequence KLIRVGIILVLLIWGTVLLLKSIPHH). The crystallized signal peptide was modified towards the LHCGR signal peptide by side-chain substitutions (sequence 7-ALQLLKLLLLLQPPLPRALR-26) and fitted it into the SRP domain M binding site (as suggested by the template) by bioinformatic methods like energy minimization and dynamic simulations.

In short, after substitution of the amino-acids from the LHCGR into the determined peptide structure, the peptide and M domain were energetically minimized until converging at a termination gradient of 0.05 kcal/mol*Å, by fixing the backbone atoms and by using the AMBER 7 force field. This step was followed by a dynamic simulation of 1.5 ns with restraint backbone atoms to justify the side-chains optimal to each other. A further dynamic simulation step was proceeded for 0.5 ns without any constraints on the protein structure. The resulting entire system was again minimized. This protocol was repeated with the bound L10P variant starting with the initial substitution step. We also performed single SP peptide modifications without the M domain. For this purpose the original SP peptide was extracted from the complex structure and the LHCGR side-chains were substituted, for wild type and the L10P mutant. The dynamic simulation (2 ns) of

the isolated peptides without backbone constraints showed generally high flexibility for both peptides (deformation of the backbone) without contacting partners. For modeling procedures the software Sybyl-X 2.0 version was used (Certara, NJ, US). Structure images were produced using the PyMOL software (The PyMOL Molecular Graphics System, Version 1.3 Schrödinger, LLC).

Acknowledgements: This work was supported by funds from University of Milan (Dotazione per attività istituzionali - Linea B Piano di Sviluppo di Ateneo) and IRCCS Istituto Auxologico Italiano (Ricerca Corrente Funds: 05C202).

Conflict of Interest Statement: All the Authors have nothing to disclose related to this manuscript.

References

1. Troppmann,B., Kleinau,G., Krause,G., and Gromoll,J. (2013) Structural and functional plasticity of the luteinizing hormone/choriogonadotrophin receptor. *Hum. Reprod. Update*, **19**, 583-602.

2. Ascoli,M., Fanelli,F., and Segaloff,D.L. (2002) The lutropin/choriocrctnadotropin receptor, a 2002 perspective. *Endocr. Rev.*, **23**, 141-174.

3. Krause,G., Kreuchwig,A., and Kleinau,G. (2012) Extended and Structurally Supported Insights into Extracellular Hormone Binding, Signal Transduction and Organization of the Thyrotropin Receptor. *Plos One*, **7**.

4. Themmen,A.P.N., Huhtaniemi,I.T. (2000) Mutations of gonadotropins and gonadotropin receptors: Elucidating the physiology and pathophysiology of pituitary-gonadal function. *Endocr. Rev.*, **21**, 551-583.

5. Huhtaniemi,I., Alevizaki,M. (2006) Gonadotrophin resistance. *Best Pract Res. Cl. En.*, **20**, 561-576.

6. Latronico,A.C., Arnhold,I.J.P. (2013) Gonadotropin resistance. *Endocr. Dev.*, **Epub**, 25-32.

7. Mitri,F., Bentov,Y., Behan,L.A., Esfandiari,N., and Casper,R.F. (2014) A novel compound heterozygous mutation of the luteinizing hormone receptor -implications for fertility. *J. Assist. Reprod. Gen.*, **31**, 787-794.

8. Newton,C.L., Whay,A.M., McArdle,C.A., Zhang,M.L., van Koppen,C.J., van de Lagemaat,R., Segaloff,D.L., and Millar,R.P. (2011) Rescue of expression and signaling of human luteinizing hormone G protein-coupled receptor mutants with an allosterically binding small-molecule agonist. *P. Natl. Acad. Sci. U.S.A.*, **108**, 7172-7176.

9. Latronico,A.C., Anasti,J., Arnhold,I.J.P., Rapaport,R., Mendonca,B.B., Bloise,W., Castro,M., Tsigos,C., and Chrousos,G.P. (1996) Testicular and ovarian resistance to luteinizing hormone caused by inactivating mutations of the luteinizing hormone-receptor gene. *New Engl. J. Med.*, **334**, 507-512.

10. Nakabayashi,K., Kudo,M., Kobilka,B., and Hsueh,A.W.J. (2000) Activation of the luteinizing hormone receptor following substitution of Ser-277 with selective hydrophobic residues in the ectodomain hinge region. *J. Biol. Chem.*, **275**, 30264-30271.

11. Bendtsen,J.D., Nielsen,H., von Heijne,G., and Brunak,S. (2004) Improved prediction of signal peptides: SignalP 3.0. *J. Mol. Biol.*, **340**, 783-795.

12. Nielsen,H., Engelbrecht,J., Brunak,S., and vonHeijne,G. (1997) Identification of prokaryotic and eukaryotic signal peptides and prediction of their cleavage sites. *Protein Eng.*, **10**, 1-6.

13. Alken,M., Rutz,C., Kochl,R., Donalies,U., Queslati,M., Furkert,J., Wietfeld,D., Hermosilla,R., Scholz,A., Beyermann,M., et al. (2005) The signal peptide of the rat corticotropin-releasing receptor 1 promotes receptor expression but is not essential for establishing a functional receptor. *Biochem. J.*, **390**, 455-464.

14. Keenan,R.J., Freymann,D.M., Walter,P., and Stroud,R.M. (1998) Crystal structure of the signal sequence binding subunit of the signal recognition particle. *Cell*, **94**, 181-191.

15. Janda,C.Y., Li,J., Oubridge,C., Hernandez,H., Robinson,C.V., and Nagai,K. (2010) Recognition of a signal peptide by the signal recognition particle. *Nature*, **465**, 507-U139.

16. Reiersen,H., Rees,A.R. (2001) The hunchback and its neighbours: proline as an environmental modulator. *Trends Biochem. Sci.*, **26**, 679-684.

17. Pietila,E.M., Tuusa,J.T., Apaja,P.M., Aatsinki,J.T., Hakalahti,A.E., Rajaniemi,H.J., and Petaja-Repo,U.E. (2005) Inefficient maturation of the rat luteinizing hormone receptor - A putative way to regulate receptor numbers at the cell surface. *J. Biol. Chem.*, **280**, 26622-26629.

18. Kochl,R., Alken,M., Rutz,C., Krause,G., Oksche,A., Rosenthal,W., and Schulein,R. (2002) The signal peptide of the G protein-coupled human endothelin B receptor is necessary for translocation of the N-terminal tail across the endoplasmic reticulum membrane. *J. Biol. Chem.*, **277**, 16131-16138.

19. Karamyshev,A.L., Patrick,A.E., Karamysheva,Z.N., Griesemer,D.S., Hudson,H., Tjon-Kon-Sang,S., Nilsson,I., Otto,H., Liu,Q.H., Rospert,S., et al. (2014) Inefficient SRP Interaction with a Nascent Chain Triggers a mRNA Quality Control Pathway. *Cell*, **156**, 146-157.

20. Walter,P., Ibrahimi,I., and Blobel,G. (1981) Translocation of proteins across the endoplasmic reticulum. I. Signal recognition protein (SRP) binds to in-vitro-assembled polysomes synthesizing secretory protein. *J. Cell Biol.*, **91**, 545-550.

21. Egea,P.F., Stroud,R.M., and Walter,P. (2005) Targeting proteins to membranes: structure of the signal recognition particle. *Curr. Opin. Struc. Biol.*, **15**, 213-220.

22. Rapoport,T.A. (2007) Protein translocation across the eukaryotic endoplasmic reticulum and bacterial plasma membranes. *Nature*, **450**, 663-669.

23. Ward,C.L., Omura,S., and Kopito,R.R. (1995) Degradation of Cftr by the Ubiquitin-Proteasome Pathway. *Cell*, **83**, 121-127.

24. Atger,M., Misrahi,M., Sar,S., Leflem,L., Dessen,P., and Milgrom,E. (1995) Structure of the Human Luteinizing-Hormone Choriogonadotropin Receptor Gene - Unusual Promoter and 5'-Noncoding-Regions. *Mol. Cell. Endocrinol.*, **111**, 113-123.

25. Bonomi,M., Busnelli,M., Persani,L., Vassart,G., and Costagliola,S. (2006) Structural differences in the hinge region of the glycoprotein hormone receptors: Evidence from the sulfated tyrosine residues. *Mol. Endocrinol.*, **20**, 3351-3363.

Legends to Figures

Fig.1. Patient phenotype and genomic analysis of the *LHCGR* gene. (A) Hormonal evaluation of proband. Reference range: (1) M.B. Ranke and P.E. Mullis, Karger, 2011. (2) W. Tabb Moore and Richard C. Eastman, Mosby, Diagnostic Endocrinology, 2° edition, 1996.(3) Segal TY, Mehta A, Anazodo A, Hindmarsh PC, Dattani MT, JCEM 2009, 94(3):780-5 (B) Histological sections of a biopsy of the patient's right testis (15 years old) at different magnifications (4x and 20x). Testis were processed for paraffin sectioning, mounted on glass slides and stained with hematoxylin and eosin by standard procedures. The Leydig cells are not visualized, and seminiferous tubules with a thick basal membrane and Sertoli cells can be seen without evidence of germinal cells. (C) DNA sequence analysis of the proband LHCGR gene.

Fig.2. Effects of the pL10P mutation on LHCGR function and expression. (A) hCG-induced cAMP produc-

tion of transiently transfected COS7 cells. cAMP response to increasing concentrations of hCG in COS7 cells transfected with constructs containing the wild type LHCGR or the p.L10P mutation is shown. B) Intracellular distribution of the wild type LHCGR or the p.L10P mutation in COS7 cells. Immunofluorescence images of fixed cells expressing the wild type LHCGR , the p.L10P and the S277L variants, captured 48h after transfection. Images are representative of three independent experiments. Scale bar, 10µm. FACS analysis of intact (C) and permeabilized (D) COS7 cells transiently transfected with the wild type LHCGR or the p.L10P and S277L variants. Results are expressed as fold of WT. (E) Ratio between membrane associated/intracellular receptors. Data are derived from FACS analysis on intact and permeabilized cells.(F) Western blot of COS7 cells transfected with WT LHCGR or the p.L10P mutation and lysed in RIPA buffer 48h post transfection. While in the LHCGR an accumulation of the two distinct species with molecular masses of 65–75 kDa, 85–95 kDa was observed, in the mutated protein we observed a faint signal (approx. 20% of the wild type) only 48h post transfection. Anti-GAPDH antibody was used as internal loading control. (G) Quantitative densitometric analysis of the blots, based on 3 different experiments (mean ±SEM). All statistical analyses were performed using Prism 5. Differences between WT and mutant receptors were tested for statistical significance by using 1-way ANOVA followed by Tukey's test (** p<0,01, *** p<0,001, ns_not significant)

Fig 3. Experimental proof of the signal peptide cleavage of LHCGR**.** (A) Depiction of the signal peptide sequences of the LHCGR receptor (upper panel) and the L10P mutant (lower panel). The probabilities of the presence of n (green), h (blue), and c (light blue) regions and the cleavage probabilities (cp, red) are indicated for each signal peptide in a score ranging from 0 to 1. (B) Representative cartoon of the fusion protein engineered between the GFP and the N-terminal domain of wild-type or mutated LHCGR and the two control receptor, CRF-R1 and CRF-R2a: the signal peptide is shown as grey box and the N-terminal domain is depicted as a black line. (C) Localization of the GFP fluorescence signals of LHCGR and its signal peptide mutant p.L10P in transiently transfected COS7 cells by confocal LSM. The corresponding constructs of the CRF-R1 and CRF-R2a receptor were used as a control for signal peptide primary functions. Scale bar, 10 µm. (D) Detection of secreted, purified constructs by immunoblotting using a monoclonal anti-GFP antibody. In each lane, the isolated protein of 4* 10^6 cells was loaded. The immuno-blot is representative of three independent experiments.

Fig.4. The structural homology model visualizes the putative general mode of binding and detailed interactions between parts of the LHCGR signal peptide (SP) and the signal recognition particle (SRP).
(A) The SRP model is subdivided into three domains (N-, G-, and M- domain) according to the determined high resolution structure (pdb code 3KL4, SRP54, bacterical SRP homologue, PMID: 20364120) that served as a structural model-template. The crystallized signal peptide was modified (side-chains were substituted) towards the LHCGR (from position Ala7 to Arg26) and fitted by energy minimization and dynamic simulations into the SRP domain M (translucent surface and backbone-ribbon presentation). Of note, we highlighted the signal peptide amino acids as lines, or in case of Leu10 (green) and the substitution L10P (cyan) as sticks. The biophysical properties of the side-chains are visualized by different colors: green-hydrophobic, red-negatively charged, orange-hydrophilic and uncharged, blue-positively charged. These colors are also visible at the M-domain surface and it reflects, therefore, complementary biophysical properties at the SRP/SP complex. (B) Western blot analysis of cells expressing the wild type LHCGR, the naturally occurring p.L10P variant or the "in silico" designed Leu10Ile (p.L10I), Leu10Ser (p.L10S), and Leu10Ala (p.L10A) variants.

Fig.5. Premature degradation of the p.L10P variant. (A) mRNA expression of LHCGR and signal peptide mutant p.L10P in transiently transfected COS7 cells by Real Time analysis. GAPDH mRNA was used to normalize template levels. Values represent the relative expression compared to controls (LHCGR/GAPDH mRNA levels). The qPCR is representative of three independent experiments. (B) Western blot analysis of cells expressing the wild type LHCGR or the p.L10P mutation treated with proteasome inhibitor MG132 for 24 hours. In cells transfected with the p.L10P mutant and treated with MG132 we observed the robust accumulation of an immature form of the LHCGR receptor (approximately 65kDa) respect to the wild type counterpart. (C) Immunofluorescence images of fixed cells expressing the WT LHCGR or the p.L10P mutation treated with proteasome inhibitor MG132 for 24 hours. Images from empty vector (pSVL) and S277L variant have been acquired as controls. Images are representative of three independent experiments. Scale bar, 10 μm. (D) The 65-kDa p.L10P species is not glycosylated, indicating a cytosolic location. COS7 cells were transfected with the wild type LHCGR or the pL10P mutation and treated with proteasome inhibitor MG132 for 24h. Protein was extracted in RIPA buffer, left untreated (−) or treated with PNGaseF, and subsequently analyzed using Western blotting.

A

Table 1. Hormonal evaluation of the patient

Variable		Reference Range (1,2,3)	12 yr	15 yr
LH (IU/L)	*Basal*	*Pre-pubertal: < 5.0* *Adult: 1.7-8.6*	10.9	40.8
	GnRH test peak	Peri-pubertal: 2-3 fold x basal Adult: 2-5 fold x basal	71.3	---
FSH (IU/L)	*Basal*	*Pre-pubertal: <5.0* *Adult: 1.5-12.4*	6.5	16.0
	GnRH test peak	Peri-pubertal: 2-3 fold x basal Adult: 1-2 fold x basal	10.4	---
T (nmol/L)	*Basal*	*Pre-pubertal* *10-11years: 0.17-1.7* *12-14 years: 0.35-19.85* *15-17 years:7.6-27.8* *Adult: 9.7-27.8*	<0.69	4.09
	hGC test peak	*>3.6*	1.49	

B

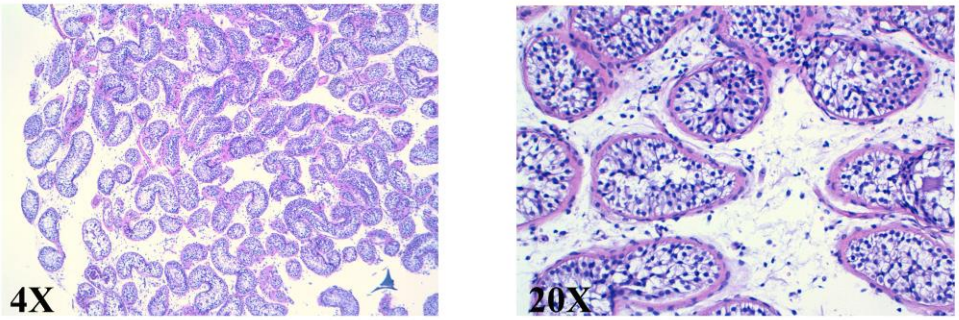

C